Some properties of milled vanadium phosphates

**Władysław Janusz · Svetlana Khalameida · Volodymyr Sydorchuk · Ewa Skwarek ·
Valery Zazhigalov · Jadwiga Skubiszewska-Zięba · Roman Leboda**

Abstract Mechanochemical modification of vanadium
phosphates doped with Bi, Zr, Mo has been studied. Milled
samples have been investigated by means of XRD, DTA-TG,
FTIR, nitrogen adsorption, electrokinetic measurements.
It was found that phase composition of the phosphates
does not change upon the mechanochemical modification
process. Milling in water causes formation of porous mate-
rials. Modification of surface results in changes of the elec-
trokinetic and adsorption properties of the milled samples.

Keywords Vanadium phosphates · Mechanochemical
treatment · Potential ζ · Ni(II) · Adsorption

1 Introduction

Acid hydrated vanadium phosphates VPO reveal ion ex-
change properties in aqueous solutions by means of sub-
stitution of proton on cation or reduction intercalation of
hydrogen or some cations into interlayer space (Yaroslavt-
sev 1997; Bruque et al. 1995; Amoros et al. 1989; Philips
et al. 1990). Particularly, vanadylhydrophosphate hemyhy-
drate VOHPO$_4$·0.5H$_2$O (VHP) can be related to phosphates
Me^{IV}(HPO$_4$)$_2$ which are typical ion exchangers (Yaroslavt-
sev 1997; Clearfield 1984). Besides, recently, vanadium
phosphates apply also as potentially very interesting ma-
trices for Li-batteries (Whittingham 2004; Kishore et al.

W. Janusz · E. Skwarek (✉) · J. Skubiszewska-Zięba · R. Leboda
Faculty of Chemistry, Maria Curie Skłodowska University,
M.C. Skłodowskiej Square 3, 20-031 Lublin, Poland
e-mail: ewunias@hermes.umcs.lublin.pl

S. Khalameida · V. Sydorchuk · V. Zazhigalov
Institute for Sorption and Problems of Endoecology NAS
of Ukraine, Naumova Street 13, 03164 Kiev, Ukraine

2006). In both cases structure of the electrical interfacial
layer in aqueous medium and its parameters play conclusive
role. Therefore, understanding of processes which take place
at the phosphates/electrolyte interface is interesting and im-
portant; in particular, the knowledge of the electrokinetic
(zeta) potential ζ of the adsorbent surface allows us to de-
termine the kind and the course of the sorption on the solid.
So, there is a correlation between ion exchange capacity and
ζ value, which is closely interrelated to the surface charge,
i.e. to the number of surface functional groups (Skwarek
and Janusz 2006). By the same token, the surface charge
at solid/electrolyte interface is formed due to the acid-base
dissociation of OH-groups.

Electrochemical properties can be characterized by the
zeta potential, which is the electrical potential of the inter-
face between volume of the aqueous solution and the sta-
tionary layer of such fluid attached to the solution cell. It
is known that Smoluchowski's formula is generally used to
determine the zeta potential of colloidal particles:

$$\zeta = \frac{\mu \eta}{\varepsilon_0 \varepsilon_r}, \tag{1}$$

where μ is the electrophoretic mobility (the electrophoretic
velocity per unit applied electric field) of particles, η is the
viscosity of the electrolyte solution, ε_r and ε_0 are the rel-
ative permittivity of the electrolyte solution and a vacuum,
respectively.

At the same time, mechanochemical treatment (MChT)
allows to activate solid and, especially, increase its dispersity
(specific surface area) and significantly change its surface
characteristics (Heinike 1984), including vanadium phos-
phates (Ji et al. 2002; Ayub et al. 2003). Therefore, the study
of interfacial processes solid/liquid for activated phosphates,
particularly VHP, in aqueous solutions of electrolytes seems
to be interesting and useful.

The purpose of this work was study of changes of phase composition, design of surface, porous structure and some electrokinetic parameters of precipitated VHP doped with Bi, Zr and Mo, and influence of their MChT (milling) in water, air, and ethanol on these properties. Besides, effect of nickel ions presence on zeta potential was determined. Choice of Ni(II) was not accidental, because it is contaminant in natural environment. Perhaps, it will be possible to use researched adsorbents for Ni(II) removal from the environment. It should be noted that only the first results are presented in this work.

2 Experimental

Pure and doped vanadium phosphates were prepared via precipitation from vanadium pentaoxide and phosphoric acid in presence of organic reducer (Ayub et al. 2003; Hutchings 2004). The typical procedure of synthesis was following: corresponding amounts of V_2O_5, oxides of metals (ratio V:P:Me = 1:1.15:0.025 for Bi or 0.1 for Zr and Mo), n-butanol and oxalic acid were refluxed with excess H_3PO_4 for 16 h at 117°C. The final solid was separated from the solution by means of filtration and heated up to 270°C in vacuum (10^{-4} Pa) for 30 h.

MChT was carried out in a planetary ball mill Pulverisette 6 (Fritsch Gmbh) for 2 h. The reaction mixture consisted of VPOBi, VPO + ZrO_2 + MoO_3 (V:Zr:Mo = 1:0.1:0.1), VPOZr(0.1) + Mo(0.1), VPOMo(0.1) + Zr(0.1). The amount of milled reagents was 10 g. XRD measurements were performed with diffractometer PW 1830 produced by Philips using CuKα radiation. To prevent the forced orientation of the crystallographic planes, samples in the form of uncompressed powders were used for the measurements. Crystallite size D_{hkl} was calculated from broadening of the most intensive reflexes using Sherrer's equation. Ratio of intensities of lines corresponding to basal and lateral planes of VHP I_{001}/I_{220} was also determined from diffractograms.

Thermogravimetric analysis was made using the Derivatograph-C (MOM, Budapest) in the temperature range 20–800°C with the heating rate 10°/min. The FTIR spectra in the range 4500–400 cm^{-1} were registered using the spectrometer "Spectrum-One" produced by Perkin–Elmer (mixtures with KBr at the mass ratio 1:20). The specific surface area S was calculated using BET method from adsorption–desorption isotherms of nitrogen ("NOVA Instruments", Quantochrome Instruments). Effective size of grains D_s was calculated in accordance with formula: $D_s = (6/\rho S) \cdot 10^3$ [nm] where ρ—density of samples, g/cm^3. Volume of mesopores V_{me} was also determined from adsorption-desorption isotherms at relative pressure of adsorbate (nitrogen) close to 1. Total pore volume V_Σ which includes

volume of meso- and macropores was determined via impregnation of samples dried at 150°C with liquid water.

The measuring of zeta potential and particle size distribution was carried out using Zetasizer 3000 (Malvern Instruments) apparatus based on photo correlation spectroscopy (PCS). The potential zeta and isoelectric point pHiep of the VPO samples has been determined as a function of pH for 0.1, 0.01 and 0.001 mol/dm^3 solutions of NaCl. The influence of ionic strength, pH, and presence of ions of Ni(II) at the VPO/NaCl solution interface was investigated. Ni ions adsorption was performed by means of radioisotope method (with ^{63}Ni isotope as a tracer) as a function of pH. The initial concentration of Ni(II) ions was 10^{-5} mol/dm^3. NaCl solution of concentration 0.01 mol/dm^3 was used as a background electrolyte.

3 Results and discussion

According to XRD data, the VHP phase forms during the synthesis of the initial VPO doped with Bi. Next MChT in water and ethanol does not change phase composition of this sample, but leads to an increase ratio of intensities I_{hkl} of two main patterns: 001 ($d = 0.571$ nm) which corresponds to basal plane, inclusive of vanalyl group V=O, and 220 ($d = 0.294$ nm) relating to the lateral plane (Bordes 1987). As can be seen from Fig. 1 and Table 1 (column 8), $I_{001}/I_{220} < 1$ for initial sample and >1 for milled samples. Thus, preferential surface exposure of basal plane with vanadyl groups V=O is observed for VPOBi undergone MChT in water and ethanol, which agrees with data of work (Zazhigalov et al. 1997). On the other hand, milling on air results in drastic amorphization of VPOBi sample (Fig. 1).

The curves of DTA-TG for initial and milled samples are presented in Fig. 2. They are typical for the phase of VHP (Cavani et al. 1985; Sidorchuk et al. 2007). The curves contain endoeffect and sharp mass loss at 350–450°C and confirm the above mentioned changes of crystal structure. Indicated mass loss for milled samples is lesser than that for initial VPOBi, which is the evidence of partial destruction of VHP phase, degree of which increases in row: ethanol–water–air.

Absorption bands (a. b.) characteristic for VHP (Johnson et al. 1984; Busca et al. 1986) are present on FTIR spectra of initial VPOBi and the sample milled in ethanol (Fig. 3).

Milling in air, which leads to the practically complete amorphization of VHP, results in loss of spectrum resolution in all studied interval. Great shift of all a. b. in the region of higher frequencies (as a rule by 15–35 cm^{-1}) and sharp decrease of their intensities are observed for the sample milled in water. Thus, a. b. at 1203 cm^{-1} (initial VPOBi) corresponding ν_sPO_3 (Busca et al. 1986) shifts towards

1291 cm^{-1} (milled sample). The latter can be explained by formation of a layer of hydrated amorphous (reprecipitated) VPO on the surface of the sample milled in water.

Crystallite size of VHP calculated on broadening of reflexes corresponding to planes 001 and 220 D_{001} and D_{220} according to Sherrer's equation is nanoscale (18–30 nm). However, crystallites are aggregated in larger grains. Excess of effective grain diameter D_s, determined from specific surface area S, over crystallite size indicates such aggregation.
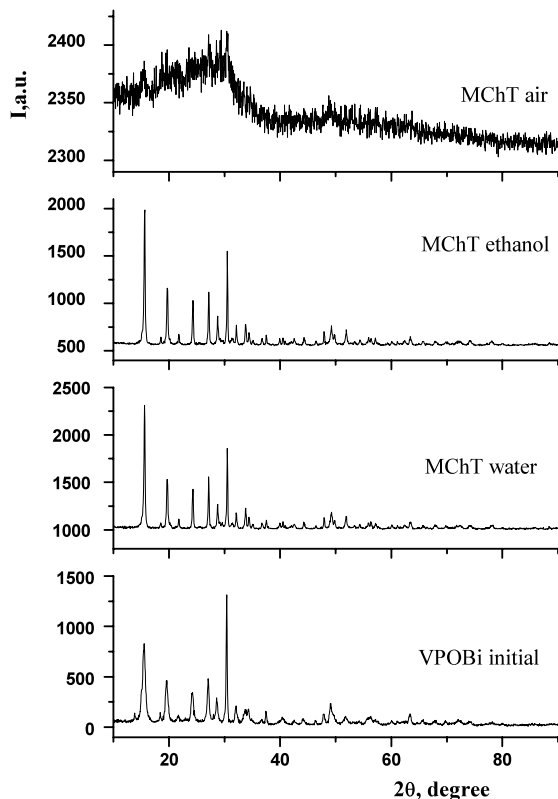
Fig. 1 Powder X-diffraction patterns for VPOBi after treatment in different media

Values of S increase after MChT in all media (Table 1, column 3). Practically nonporous initial VPOBi turns into porous substance due to milling in water: total pore volume $V_\Sigma = 0.39$ cm^3/g, pore volume of mesopores—0.03 cm^3/g, macrospores—0.36 cm^3/g.

Similar changes are observed during doping VPO with zirconium and molybdenum oxides via MChT in ethanol. XRD data (Fig. 4) indicate that initial VPO (diffractogram a), VPO doped with Mo or Zr during precipitation (diffractogram does not presented), VPO doped with (MoO$_3$ + ZrO$_2$) via milling (b), and VPOZr doped with MoO$_3$ via milling (c) possess structure of VHP with $I_{001}/I_{220} = 1.25$. Diffractogram of VPOMo undergone MChT with ZrO$_2$ is superposition of phases of VHP and zirconium pyrophosphate. Diffractogram of this sample (strong background and small intensities of all patterns) evidences that amorphization occurs during milling. FTIR spectra of indicated samples (Fig. 5) confirm above mentioned assumptions.

From Table 1 (samples 5–10) one can see that value of S slightly decreases at dopation of VPO on stage of precipitation and sharply decreases during MChT of VPO with (ZrO$_2$ + MoO$_3$) or VPOMo with Zr. On the contrary, specific surface area of VPOZr increases substantially after its milling with MoO$_3$.

In Table 2, value of particles size determined via electroforethic measurements and pH$_{iep}$ values for different adsorbents are presented. One can see dependence between particles size (Table 2) and specific surface area S (Table 1): the bigger the particles are, the smaller the S is. In all cases pH$_{iep}$ value is around 2, except for initial VPOBi, for which pH$_{iep} > 3$. This indicates the negative charge of the surface.

Figure 6 shows zeta potential as a function of pH for the system: VPOBi modified in different media/0.001 mol/dm^3 NaCl/0.0001 mol/dm^3 Ni. Zeta potential of all samples in the studied range pH is negative and decreases with the solution pH increase. At the same time, ζ value achieves local minimum at pH = 5.5 (and at pH = 7 for sample milled in air) and increases in region of higher pH. As can be seen

Table 1 Some properties of VPO samples milled in different media

N	Samples, conditions of MChT	S (m^2/g)	V_Σ (cm^3/g)	D_s (nm)	D_{001} (nm)	D_{220} (nm)	I_{001}/I_{220}
1	VPOBi initial	5	0.01	310	18.3	21.3	0.64
2	+ MCHT ethanol 2 h	11	0.03	140	25.0	30.6	1.27
3	+ MCHT water 2 h	10	0.39	155	22.9	27.8	1.25
4	+ MCHT air 2 h	8	0.02	195	–	–	–
5	VPO initial	19	–	80	21.5	25.8	0.68
6	+ MChT ethanol 2 h with MoO$_3$(0.1) + ZrO$_2$(0.1)	5	–	265	15.4	31.4	1.25
7	VPOMo(0.1) initial	14	–	105	22.3	26.0	0.72
8	+ MChT ethanol 2 h with ZrO$_2$(0.1)	7	0.37	190	15.5	16.5	1.25
9	VPOZr(0.1) initial	16	–	95	21.6	24.9	0.71
10	+ MChT ethanol 2 h with MoO$_3$(0.1)	38	0.53	35	13.8	26.6	1.25

Fig. 2 TG-DTA curves for
initial and milled VPOBi
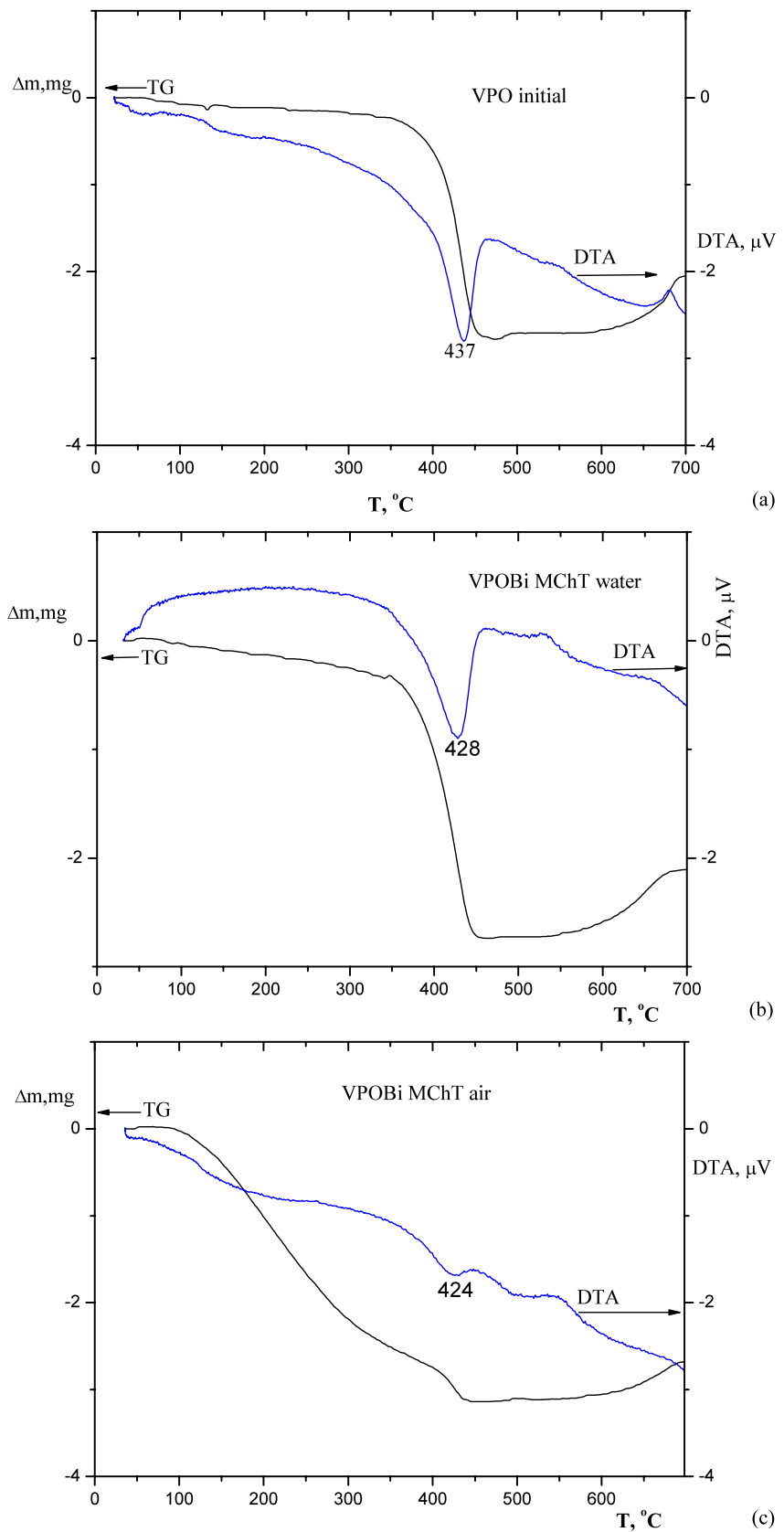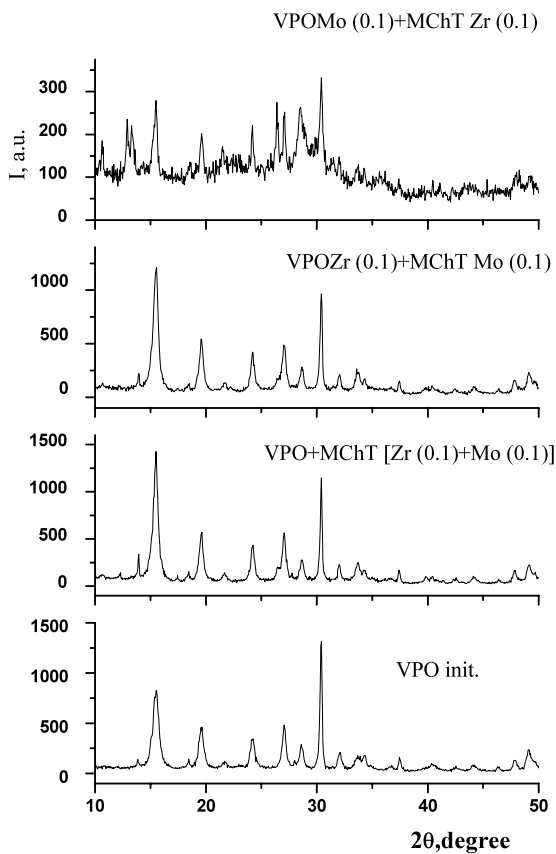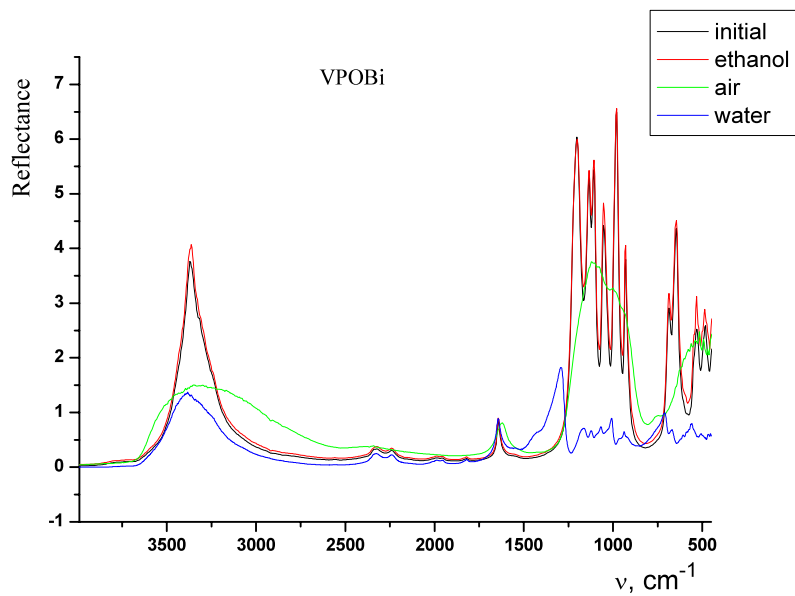
scribed for higher content of Ni and other ions (Skwarek and Janusz 2006; Hunter and James 1992; Kuan et al. 2004). One can see that the samples treated in water and ethanol have close values of specific surface area. Similar changes of zeta potential as a function of pH are observed for them. Such behavior of these samples may be the result of reactions occurring in the system during milling, i.e. dissociative adsorption of ethanol and water at their surface.

Figure 7 shows the influence of the presence of Ni on zeta potential depending on pH for VPO samples doped with Mo and Zr on precipitation and milling stages. Similar to samples doped with Bi, the increase of zeta potential at pH > 6 occurs, but less significant than in case of VPOBi samples.

The example of Ni(II) ions adsorption as a function of pH in the VPOBi/NaCl solution system is presented in Fig. 8. This is the sample milled in water. It was found that the adsorption edge of the nickel ions in the studied system increases with increase of pH values. At pH > 6.5, the adsorption remains the same, because almost all nickel ions are bonded by solid phase. Similar isotherm was obtained for VPOBi milled in ethanol. However, sample milled in air does not adsorb Ni ions when their concentration equals 0.00001 mol/dm^3. The latter can be explained by amorphization of VPOBi during dry mechanochemical treatment. Therefore, only crystal VPO, namely acid hydrophosphate phase, possesses ion exchange properties.

Electrokinetic and adsorption properties of milled vanadium phosphates obviously are determined by their crystal structure and surface design, particularly, appearance of structure defects and greater number of surface hydroxyl groups. However, the relationship of these characteristics is rather complicated. Therefore, additional studies are required for its establishment.

from Fig. 6, overcharging of the diffuse layer, which is associated with Ni ions adsorption, does not occur in the presence of nickel with concentration 0.0001 mol/dm^3. Therefore, a charge reversal point (CR2) is not observed, as de-
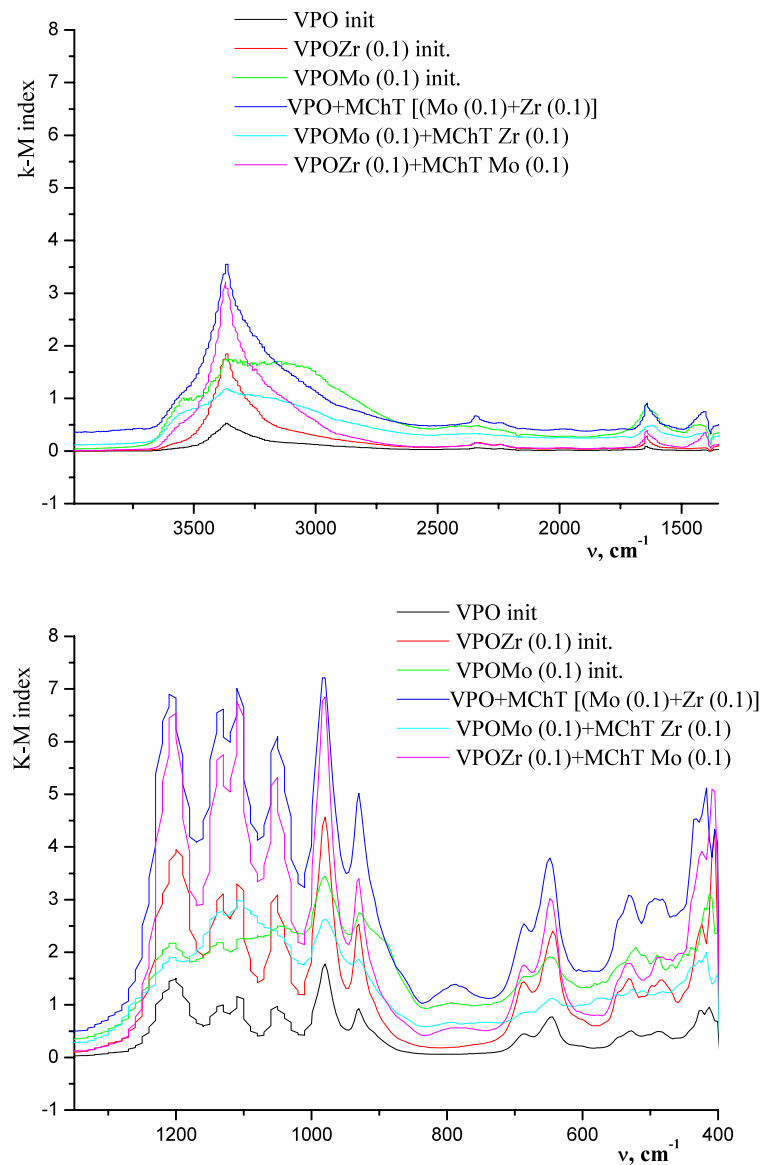
Fig. 5 FTIR spectra for samples doped with Mo and Zr

Table 2 Size of particles and pH$_{iep}$ for initial and milled samples

N	Samples, conditions of MChT	Particles size (nm)	pH$_{IEP}$
1	VPOBi initial	709	<3
2	+ MCHT ethanol 2 h	568	2
3	+ MCHT water 2 h	653	2
4	+ MCHT air 2 h	684	2
5	VPO initial	316	2
6	+ MChT ethanol 2 h with MoO$_3$ (0.1) + ZrO$_2$(0.1)	712	<2
7	VPOMo(0.1) initial	443	<2
8	+ MChT ethanol 2 h with ZrO$_2$(0.1)	692	<2
9	VPOZr(0.1) initial	332	<2
10	+ MChT ethanol 2 h with MoO$_3$(0.1)	235	<2

Fig. 6 ζ potential at
VPOBi/NaCl/0.0001 mol/dm^3
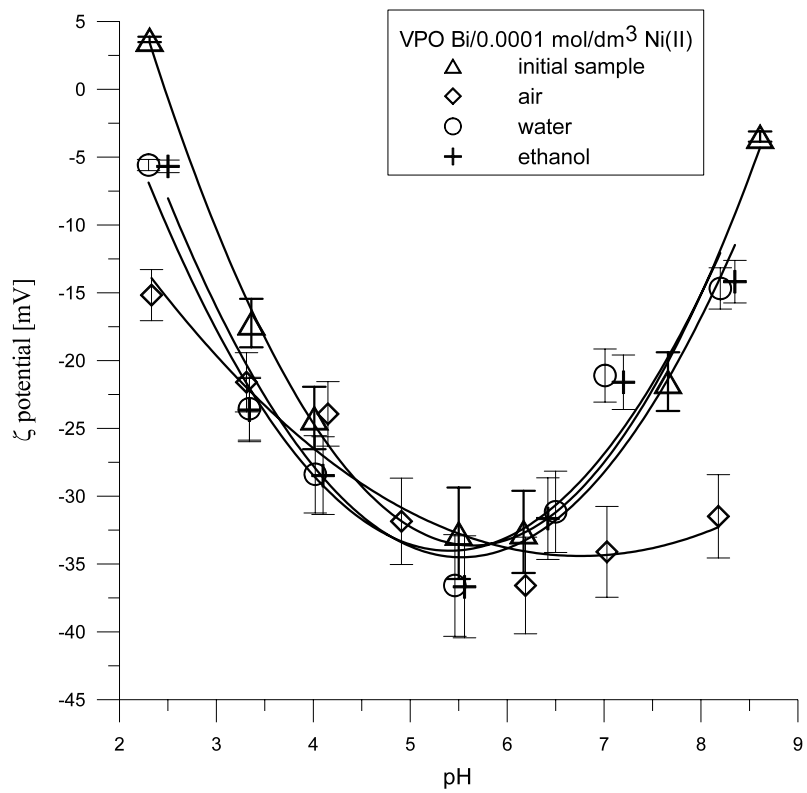Ni(II) solution interface as a
function pH

Fig. 7 ζ potential at
samples/NaCl/0.0001 mol/dm^3
Ni(II) solution interface as a
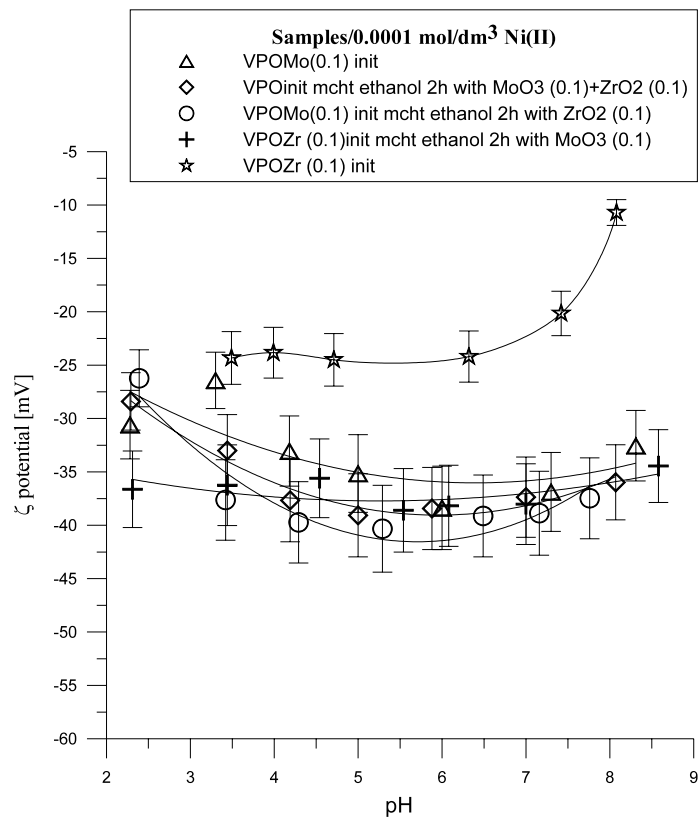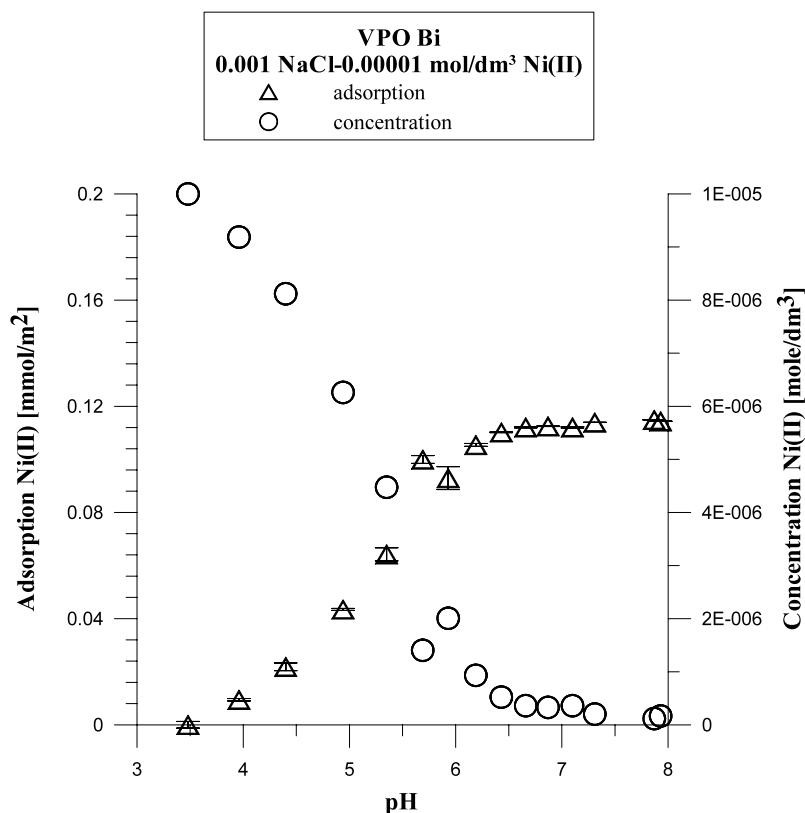function pH

Fig. 8 Adsorption of Ni VPO
Bi/NaCl/0.00001 mol/dm^3
Ni(II) solution interface as a
function pH

4 Conclusions

Mechanochemical treatment of the VPO samples has influence on the surface properties, which was shown by means of XRD, IR, TG-DTA investigations. It was established that their phase composition does not change when milling takes place in water and ethanol, but dry milling results in significant destruction of crystal structure (amorphization). At the same time, noticeable change of preferential orientation of main crystallographic planes occurs: surface content of basal plane sharply increases for all milled samples (except sample prepared via dry milling). The latter and the fact of increase of hydroxyl groups content significantly modify surface design. Presence of Ni cations with concentration 0.0001 mol/dm^3 does not cause overcharging of the diffuse layer. Destruction of crystal structure of vanadylhydrophosphate during mechanochemical treatment in air results in change of type of dependence "zeta potential–pH" and loss of adsorption capacity. Formation of porous samples during milling in liquid media (water and ethanol) was also established. At the same time, the samples remain nonporous as a result of dry milling in air.

References

Amoros, P., Ibanez, R., Martinez, E., Beltran-Porter, A., Beltran-Porter, D., Villeneuve, G.: New vanadyl hydrogenphosphate hydrates: electronic spectra of the VO^{2+} ion in the $VO(H_xPO_4)_x \cdot yH_2O$ system. Mater. Res. Bull. **24**, 1347–1360 (1989)

Ayub, I., Su, D., Willinger, M., Kharlamov, A., Ushkalov, L., Zazhigalov, V., Kirillova, N., Schlögl, R.: Tribomechanical modification of Bi promoted vanadyl phosphate systems 1: an improved catalyst and insight into structure–function relationship. Phys. Chem. Chem. Phys. **5**, 970–977 (2003)

Bordes, E.: Crystallochemistry of V-P-O phases and application to catalysis. Catal. Today **1**, 499–526 (1987)

Bruque, S., Lara, M.M., Moreno, L., Ramirezcardenas, T., Chaboy, J., Marziali, M., Stizza, S.: EXAFS structure and electrical properties of lithium niobium phosphate. J. Solid State Chem. **114**, 317–325 (1995)

Busca, G., Cavani, F., Centi, G., Trifiro, F.: Nature and mechanism of formation of vanadyl pyrophosphate: active phase in n-butane selective oxidation. J. Catal. **99**, 400–414 (1986)

Cavani, F., Centi, G., Trifiro, F., Poli, G.: Structure and reactivity of vanadium-phosphorus oxides. J. Therm. Anal. **30**, 1241–1251 (1985)

Clearfield, A.: Inorganic ion exchangers with layered structure. Annu. Rev Mater. Sci. **14**, 205–229 (1984)

Heinike, G.: Tribochemistry. Akademie-Verlag, Berlin (1984)

Hunter, R.J., James, M.: Charge reversal of kaolinite by hydrolyzable metal ions: an electroacoustic study. Clays Clay Miner. **40**, 644–649 (1992)

Hutchings, G.J.: Vanadium phosphate: a new look at the active components of catalysts for the oxidation of butane to maleic anhydride. J. Mater. Chem. **14**, 3385–3395 (2004)

Ji, W., Xu, L., Wang, X., Hu, Z., Yan, Q., Chen, Y.: Effect of ball milling on the doped vanadium phosphorus oxide catalysts. Catal. Today **74**, 101–106 (2002)

Johnson, J.W., Jacobson, J., Brody, J.F.: Preparation and characterization of vanadyl hydrogen phosphate hemihydrate and its topotactic transformation to vanadyl pyrophosphate. J. Am. Chem. Soc. **106**, 8123–8128 (1984)

Kishore, M.S., Pralong, V., Caignaert, V., Varadaraju, U.V., Raveau, B.: Synthesis and electrochemical properties of a new vanadyl phosphate: $Li_4VO(PO_4)_2$. Electrochem. Commun. **8**, 1558–1563 (2006)

Kuan, W.H., Lo, S.L., Wang, M.K.: Modeling and electrokinetic evidences on the processes of the Al(III) sorption continuum in $SiO_{2(s)}$ suspension. J. Colloid Interface Sci. **272**, 489–497 (2004)

Philips, M.L.F., Harrison, W.T.A., Gier, T.E., Stuchi, G.D., Kulkarni, G.V., Burdett, J.K.: Electronic effects of substitution chemistry in the potassium titanyl phosphate ($KTiOPO_4$) structure field: structure and optical properties of potassium vanadyl phosphate. Inorg. Chem. **29**, 2158–2163 (1990)

Sidorchuk, V.V., Diyuk, E.A., Zazhigalov, V.A.: Phase evolution in $V_2O_5-H_3PO_4-$organic component systems during barothermal treatment. Inorg. Mater. **43**, 406–411 (2007)

Skwarek, E., Janusz, W.: Adsorption of Ni(II) ions at the Fe_2TiO_5/electrolyte solution interface—the electrical double layer structure. Physicochem. Probl. Miner. Process. **40**, 149–159 (2006)

Whittingham, M.S.: Lithium batteries and cathode materials. Chem. Rev. **104**, 4271–4290 (2004)

Yaroslavtsev, A.B.: Ion exchange in the inorganic sorbents. Russ. Chem. Rev. **66**, 579–596 (1997)

Zazhigalov, V., Haber, J., Stoch, J., Kharlamov, A.: Influence of the mechanochemical treatment on the reactivity of V-containing oxide systems. Solid State Ionics **101–103**, 1257–1262 (1997)